Obstacle avoidance for an autonomous vehicle using force field method

B.Mashadi[a*], M.A.Vesal[a], H.Amani[a]

[a] School of Automotive Engineering, Iran University of Science and Technology, P.O.B. 16846-13114, Farjam st, Tehran, Iran,

b_mashhadi@iust.ac.ir

Abstract

This paper presents a force field concept for guiding a vehicle at a high speed maneuver. This method is similar to potential field method. In this paper, motion constrains like vehicles velocity, distance to obstacle and tire conditions and such lane change conditions as zero slop condition and zero lateral acceleration are discussed. After that, possible equations as vehicles path are investigated. Comparing advantages and disadvantages of 7th, 11th degree and a few other equations, followed by single mass and bicycle models lead to an improved method, which is presented in this paper.

Keywords: Potential field, Force field, Lateral acceleration, Tire stiffness, Obstacle avoidance

1. Introduction

In recent decades advanced technologies for active vehicle safety have become very popular and implemented in road vehicles. Automatic or assisted braking, adaptive cruise control, lane departure warning, and collision warning systems are among many available safety options [1]. New options such as lane departure control, active steering, automatic lane change and automatic collision avoidance, reveals the need for active systems to perform the required maneuvers to avoid a crash. Such maneuvers require two main functions: a planned trajectory for the vehicle to follow and a controller to guide the vehicle to safely traverse the planned trajectory. When there is an eminent collision situation, the vehicle often has a high speed and integrated lateral-longitudinal control motion needs to be performed in a very short period of time.

Active steering can be found in some vehicle models in the form of lane keeping systems [2]. Many researchers have investigated active steering and control systems, both linear and nonlinear to perform an automated lane change maneuver or evasive maneuvers [3-5]. Different strategies for lane change maneuver using a 5th order polynomial is studied in [9]. In [10] and [11] a model predictive control strategy was investigated to follow a desired trajectory.

A method with similarities to the concept introduced in this paper is called the potential field. This method is gaining more interest in obstacle avoidance applications for mobile robots and manipulators. The heart of this analysis is a differential equation that combines the robot and the environment into a unified system. Even though the main advantage of the potential field principle is its simplicity and performance, there are some essential shortcomings attributed to this method that are inherent to this principle [15]. An evolutionary artificial potential field method called grid method was introduced to optimize obstacle avoidance path. The simulation results showed the effectiveness of the method [16]. As a result of direct control of steering, this approach is well suited to local navigation for nonholonomic robots. The resulting paths are smooth and have continuous curvature. This approach is designed to be used with single-camera vision without depth information in first place but can also is applicable with other kinds of sensors. The suggested method is implemented and tested on a differential-drive robot and the experimental results are presented [17]. Traditional artificial potential field method might be trapped in a local minimum blocking its application and performance in real-time mobile robot path planning, security and accessibility in dynamic environment. In order to obviate this problem a new method is developed by: are introduced: taking the advantage of velocity vector, modifying potential field force function, and integrating with the fuzzy

control method and adjusting the factors of repulsion potential field in real time [18]. A proposed algorithm is developed based on new potential functions using the distances from obstacles, destination point and start point, while keeping the simplicity of traditional APF methods,. The algorithm uses the potential field values iteratively to find the optimum points in the workspace in order to form the path from start to destination [19]. In Ref. [20], an improved artificial potential field based regression search (Improved APF-based RS) method is developed, which can obtain a global sub-optimal/optimal path efficiently without local minima and oscillations in complete known environment information. Potential functions are redefined to eliminate non-reachable and local minima problems, and utilize virtual local target for robot to escape oscillations. As the planned path by improved APF is not the shortest/approximate shortest trajectory, we develop a regression search (RS) method to optimize the planned path. The optimization path is calculated by connecting the sequential points, which are produced by improved APF. Amount of simulations demonstrate that the improved APF method very easily escape from local minima and oscillatory movements. An approach witch deals with the navigation of a mobile robot in an unknown environment is developed based on the Artificial Potential Field (APF) method in which the target creates a virtual potential that attracts the robot while obstacles create a virtual potential that repels the robot. A new form of repelling potential is proposed in order to reduce oscillations and to avoid conflicts when the target is close to obstacles. A rotational force is integrated as well, allowing for a smoother trajectory around the obstacles. The results of experiments show the effectiveness of the proposed approach [21]. Using the mobile robot dynamic characteristics of the working environment, a model based on classic artificial potential field on the basis of considering dynamic model of velocity potential field is presented and simulation results show that this method can effectively improve the performance of path planning [22].

Another method is presented to represent complex shaped obstacles in harmonic potential fields used for vehicle path planning. The proposed method involves calculating the potential field for a series of circular obstacles inserted into the unobstructed potential field. The potential field for the total obstacle is a weighted average of the circular obstacle potential fields. This method explicitly calculates a stream function for the potential field. The need for the stream function is explained for situations involving controlling a dynamic system such as a high speed ground vehicle. The traditional potential field controller is also augmented to take the stream function into account. Simulation results are presented to show the effectiveness of the potential field generation technique and the augmented vehicle controller [23]. A new concept using a virtual obstacle is proposed to escape local minimums occurred in local path planning. A virtual obstacle is located around local minimums to repel a mobile robot from local minimums. A sensor based discrete modeling method is also proposed for modeling of the mobile robot with range sensors. This modeling method is adaptable for a real-time path planning because it provides lower complexity [24]. A path-planning algorithm for the classical mover's problem in three dimensions using a potential field representation of obstacles is presented. A potential function similar to the electrostatic potential is assigned to each obstacle, and the topological structure of the free space is derived in the form of minimum potential valleys. Path planning is done at two levels. First, a global planner selects a robot's path from the minimum potential valleys and its orientations along the path that minimize a heuristic estimate of the path length and the chance of collision. Then, a local planner modifies the path and orientations to derive the final collision-free path and orientations. If the local planner fails, a new path and orientations are selected by the global planner and subsequently examined by the local planner. This process is continued until a solution is found or there are no paths left to be examined. The algorithm solves a much wider class of problems than other heuristic algorithms and at the same time runs much faster than exact algorithms [25]. The potential field method is widely used for autonomous mobile robot path planning due to its elegant mathematical analysis and simplicity. However, most researches have been focused on solving the motion planning problem in a stationary environment where both targets and obstacles are stationary. Ref. [26] proposes a new potential field method for motion planning of mobile robots in a dynamic environment where the target and the obstacles are moving. Firstly, the new potential function and the corresponding virtual force are defined. Then, the problem of local minima is discussed. Finally, extensive computer simulations and hardware experiments are carried out to demonstrate the effectiveness of the dynamic motion planning schemes based on the new potential field method.

In potential field method, vehicle (or any other moving object) is considered as a single particle. This method is mostly used for small particles which have

no roll, pitch or yaw angle. On the other hand force field needs to at least consider yaw angle because it is very important in vehicle stability. Pitch and roll angles also affect vehicle stability. This paper investigates the effect of yaw angle on stability.

Moreover, potential field considers vehicle and target as particles with opposite electric charge, however in force field method the vehicle has no load and field guides the vehicle to move toward target. So, main difference between force field and potential field is vehicle and robot dimensions because roll, pitch and yaw angles are ignorable for a small object. Huge difference between vehicle and robot velocity is another discrepancy of potential field and force field.

In this paper, a force field method is used to guide a vehicle. Motion constrains and lane change conditions are discussed in the opening chapters. After that a single mass model, bicycle model and a developed model are developed and results for discussed models are compared.

2. Force field definition and motion constrains

According to Newton's second law, applying a force to a particle produces acceleration in the direction of the force. This acceleration changes velocity and displaces the particle. On the other hand, applying a moment on a rigid body produces an angular acceleration which in turn changes the angular velocity of the body. These definitions are the basic concepts of the force field concept. Force field has some similarities to the potential field discussed in the introduction. Consider a vehicle that needs to change the lane to avoid collision with an obstacle. During this lane change maneuver, the vehicle center of mass moves in forward and lateral directions. For matching orientation, the vehicle body also needs to rotate. So the vehicle is under a variable force and moment field. Values of the force and moment depend on obstacles dimensions and vehicle's weight, inertia, dimensions and velocity.

In a real vehicle, an input steer angle produces tire slip angles and in turn lateral force by tires and the vehicle starts to have lateral and angular movements. In the force field concept, however, the vehicle receives the required force (and moment) for the maneuver from the force field around the obstacle, causing the vehicle to move in longitudinal and lateral directions, and also undergo angular rotations. With this concept, the vehicle is assumed to be a rigid body with mass and inertia, that has no contact with the ground and the force (and moment) is applied from the external field.

2.1. Motion constrains

A vehicle needs to choose a path that satisfies motion constrains while passing an obstacle. Lateral acceleration is the most important factor that influences vehicle's stability. In this part, vehicle's dynamic parameters that influence lateral acceleration are explained.

2.1.1. Vehicle velocity

According to equation 1, following a specific path is more difficult in a higher velocity. The reason is that lateral acceleration increases by velocity squared.

$$a_y = \frac{V^2}{\rho}$$

where a_y is lateral acceleration and ρ and V are path curvature and velocity respectively. Equation 1 on the other hand shows that the path curvature also affects the lateral acceleration. A higher path curvature leads to a lower lateral acceleration and makes it easier for the vehicle to stay on the path.

2.1.2. Distance to obstacle

Distance to obstacle is important when the vehicle undergoes a lane change to pass an obstacle. In a close distance, the vehicle needs a higher lateral acceleration to pass the obstacle because the vehicle with a given speed, needs a smaller radius of turn.

2.1.3. Obstacle width

Obstacle width determines the amount of vehicle lateral displacement to pass the obstacle. The obstacle width is considered as lateral distance between edge of the obstacle and one side of the vehicle as shown in figure 1.

2.1.4. Tire-road friction coefficient

The amount of friction force between tires and road plays the most important role in vehicle maneuver and avoiding obstacles. The type of road and environmental situations such as rain and snow are very influential on the tire-road friction coefficient.

2.1.5. Tire lateral force

Tire lateral force generation is important in maneuverability and avoiding obstacles. Figure 2 shows the relation between force and lateral slip. Tire lateral slip is defined according to equations 2 and 3 for a two-wheel vehicle.
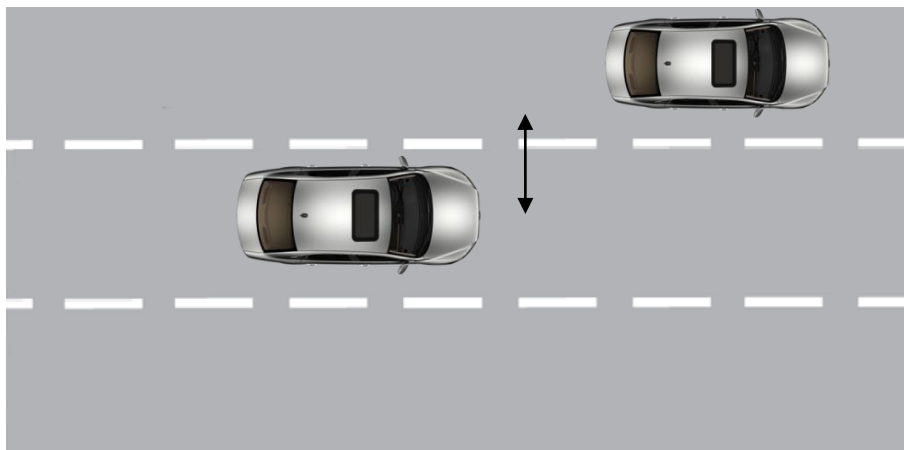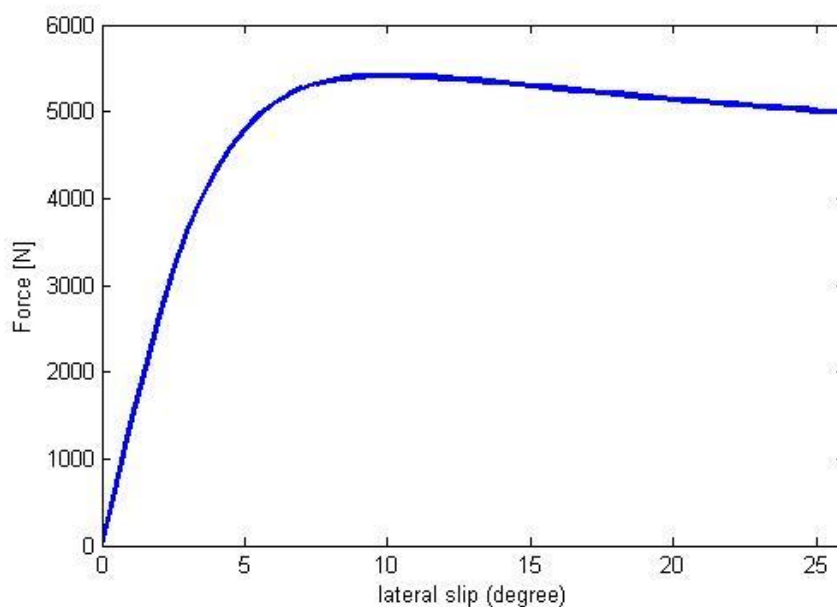
Fig1. Obstacle width

Fig2.: Tire force versus lateral slip at a given normal load

$$\alpha_f = \tan^{-1} \frac{v + ar}{U} - \delta$$
$$\alpha_r = \tan^{-1} \frac{v - br}{U}$$

where α_f is front wheel slip, α_r is rear wheel slip, r is vehicle yaw rate around vertical axis, U is vehicle longitudinal speed and δ is front steer angle. a and b, are distances between center of mass and front and rear axle respectively. During a turn, vehicle lateral slip is typically positive at low speeds and becomes negative at high speeds.

Tire cornering stiffness is the slope of tire force-slip curve. For low lateral accelerations, the linear part of diagram of Figure 2 determines the tire cornering stiffness. A higher cornering stiffness means a higher lateral force is generated for given vertical force and slip angle.

3. A single mass model

In this part, the vehicle is assumed to be a single mass object, and a force field is defined for it. For a single mass vehicle, force field condition should guide the vehicle through a lane change to avoid collision with obstacles. Longitudinal velocity is

assumed to remain constant, so the longitudinal acceleration and longitudinal force is zero and lateral force is derived from lateral acceleration.

Dynamic conditions for the lane change can be described by mathematical equations. Figure 5 shows a typical lane change path for a vehicle. According to figure 5, the lateral conditions are,

$$y(0) = 0$$
$$y(L) = W$$

The vehicle needs to move in longitudinal direction with no lateral velocity and acceleration at beginning and end of the path. The slope of curve must be zero at these points,

$$y'(0) = 0$$
$$y'(L) = 0$$

The vehicle has no lateral acceleration during pure longitudinal motion. So lateral acceleration equals zero at the beginning and end of the path. The path curvature in general is described by,

$$\rho = \frac{\left(1 + y'^2\right)^{3/2}}{y''}$$

where y' and y'' are first derivative and second derivative of y in terms of x. Because of zero lateral acceleration condition, path curvature is infinite at beginning and end of the path. Therefore,

$$y''(0) = 0$$
$$y''(L) = 0$$

Like previous conditions, the vehicle produces no turning moment during forward movement. So moment around the vertical axis equals zero at the beginning and end of the path. The path angle is,

$$\Psi = tan^{-1} y'$$

where $\dot{\Psi}$ and $\ddot{\Psi}$ are derivatives of Ψ that indicates angular speed (also denoted by r) and angular acceleration (also denoted by α) respectively. Differentiation leads to,

$$\dot{\Psi} = \dot{y}' \left(\frac{1}{y'^2 + 1}\right)$$

$$\ddot{\Psi} = \ddot{y}' \left(\frac{1}{y'^2 + 1}\right) - \frac{2y'\dot{y}'^2}{(y'^2 + 1)^2}$$

With zero slip condition, torque is calculable using equation 8. y' and $\dot{y}'$ are zero at beginning and end of the path, so $\ddot{y}'$ is also zero.

$$\dot{\Psi} = \dot{y}' \left(\frac{1}{y'^2 + 1}\right)$$

$$\ddot{\Psi} = \ddot{y}' \left(\frac{1}{y'^2 + 1}\right) - \frac{2y'\dot{y}'^2}{(y'^2 + 1)^2}$$

$$\ddot{y}'(0) = 0$$
$$\ddot{y}'(L) = 0$$

These four conditions are needed for avoiding an obstacle, but there are more circumstances that have to be investigated.

3.1. Force field development

This part discusses possible force fields suitable for using as a lane change path. Any potential force field must satisfy the above conditions. Polynomials are simple choices for this purpose, and 7th order and higher order equations satisfy all above conditions. In order to show the effect of complexity, two cases of 7th and 11th order models will be discussed here

3.1.1. 7 the order equation

A 7th order equation has in general, 7 coefficients that can be obtained by using the available conditions. Applying the boundary conditions to a 7th order equation for the vehicle path results in:
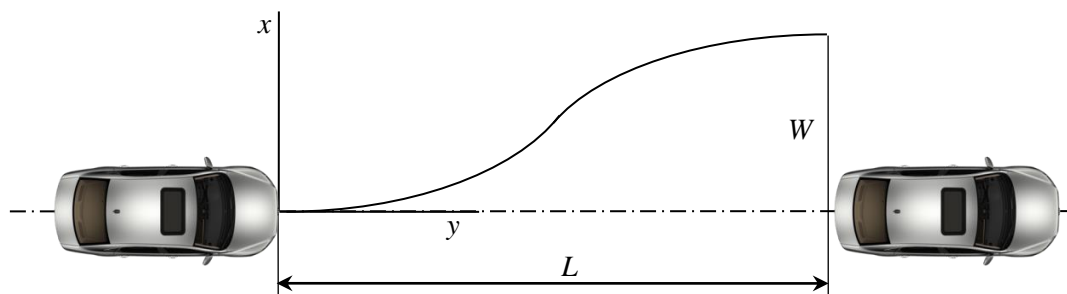

Fig3.- Vehicle lane change path definition

$$y = W\left(\frac{35x^4}{L^4} - \frac{84x^5}{L^5} + \frac{70x^6}{L^6} - \frac{20x^7}{L^7}\right)$$

or a single mass vehicle, during a constant speed lane change maneuver the lateral acceleration a_y can be obtained by making use of Eqs. 1, 6 and 14,

$$a_y = \frac{420V^2Wx^2(L-x)^2(L-2x)}{L^7\left(\frac{19600W^2x^6(L-x)^6}{L^{14}} + 1\right)^{\frac{3}{2}}}$$

Multiplying acceleration by the vehicle mass M and calculating x and y components of it results in the force field components in x and y directions.

$$F_y = m\frac{420V^2Wx^2(L-x)^2(L-2x)}{L^7\left(\frac{19600W^2x^6(L-x)^6}{L^{14}} + 1\right)^{\frac{3}{2}}}\cos(\Psi)$$

$$F_x = m\frac{420V^2Wx^2(L-x)^2(L-2x)}{L^7\left(\frac{19600W^2x^6(L-x)^6}{L^{14}} + 1\right)^{\frac{3}{2}}}\sin(\Psi)$$

Where F_x and F_y are the force field components developed in *x* and *y* directions respectively. The force field accompanies a moment that is responsible for the rotation of the vehicle body. Similar to the force concept, then angular acceleration times the vehicle body inertia produces calculated the moment filed. The angular acceleration of the vehicle during a lane change maneuver is:

$$\ddot{\Psi} = \ddot{x}(42a_7x^5 + 30a_6x^4 + 20a_5x^3 + 12a_4x^2 + 6a_3x) + \dot{x}^2(210a_7x^4 + 120a_6x^3 + 60a_5x^2 + 24a_4x + 6a_3)$$

For a constant longitudinal speed $\ddot{x} = 0$, $\dot{x} = V$ and thus the yaw moment around the vehicle vertical axis is,

$$M = I_zV^2(210a_7x^4 + 120a_6x^3 + 60a_5x^2 + 24a_4x + 6a_3)$$

3.1.2. 11th order equation

An 11th degree equation is used as a path with higher flexibility and the results are compared with those of the 7th degree equation. Relevant equations for this case are,

$$y = W\left(\frac{462x^6}{L^6} - \frac{1980x^7}{L^7} + \frac{3465x^8}{L^8} - \frac{3080x^9}{L^9} + \frac{1386x^{10}}{L^{10}} - \frac{252x^{11}}{L^{11}}\right)$$

$$F_y = \frac{13860V^2Wx^4(L-x)^4(L-2x)}{L^{11}\left(\frac{7683984W^2x^{10}(L-x)^{10}}{L^{22}} + 1\right)^{\frac{3}{2}}}\cos(\Psi)$$

$$F_x = \frac{13860V^2Wx^4(L-x)^4(L-2x)}{L^{11}\left(\frac{7683984W^2x^{10}(L-x)^{10}}{L^{22}} + 1\right)^{\frac{3}{2}}}\sin(\Psi)$$

$$M = \frac{1}{L^{11}}27720I_zV^2Wx^3(L-x)^3(L-3x)(2L-3x)$$

In figures 11 to 14 the results obtained for both 7th degree path and 11th degree path are compared for the numerical values of $W = 4$ m , $L = 50$ m, $m = 1200$ kg , $I_z = 750$ kgm^2 and $V = 20$ m/s . Quite large differences can be seen between the results of the two models. The 11th degree path has lower curvatures and as a result higher lateral accelerations and force fields.

Moment field is plotted in figure 10 for the conditions which lateral slip is neglected and vehicles moves considered to be along the path.
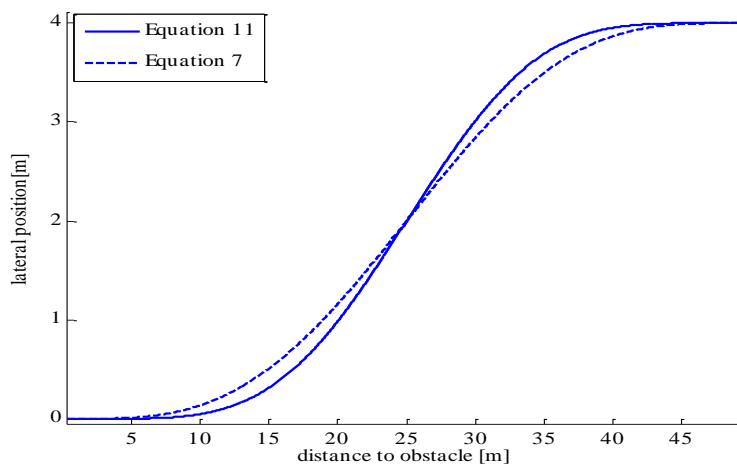

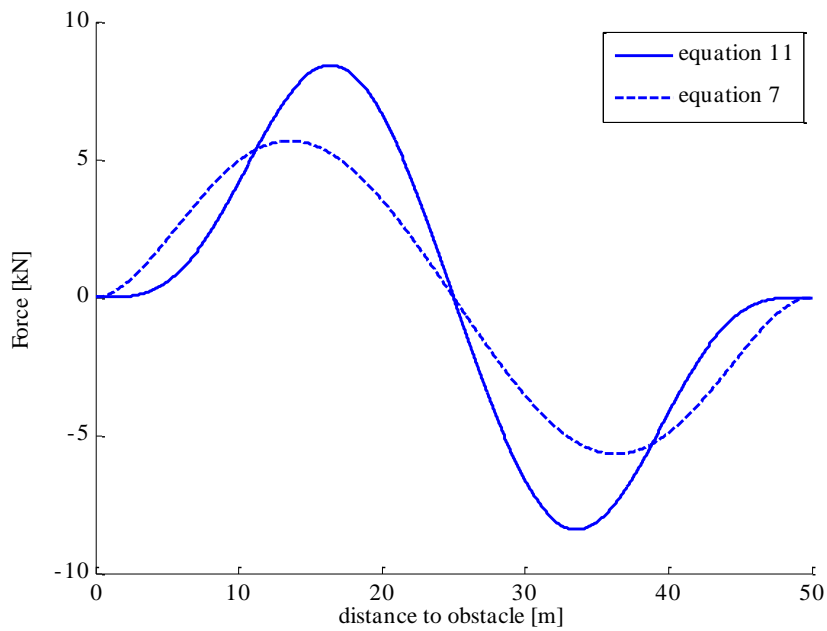**Fig4.** Lane change path comparison for 7th degree and 11th degree paths

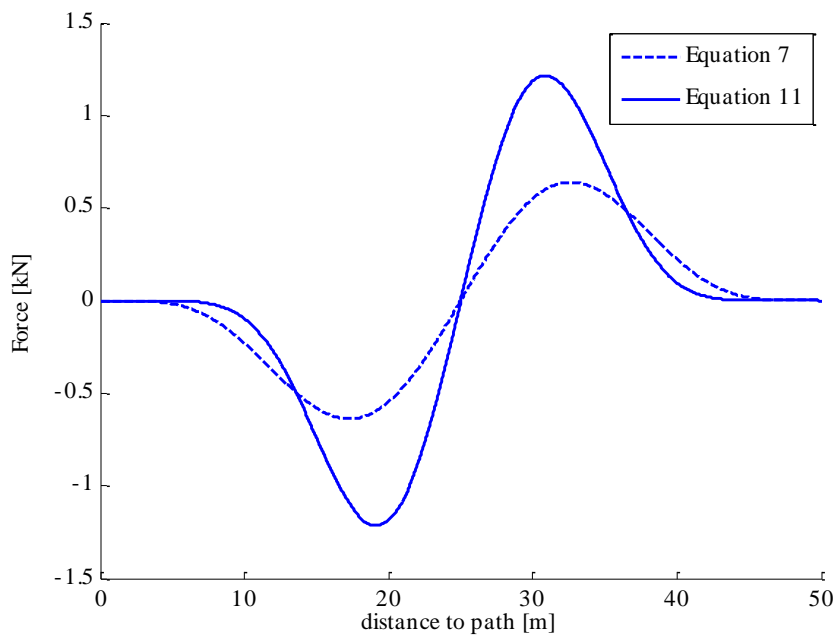**Fig5.** Lateral force field comparison for 7th degree and 11th degree paths

Fig6. Longitudinal force field comparison for 7th degree and 11th degree paths

3.1.3. Other models

Many other equations can be used as a path such as *tanh* and tan^{-1} and e^x functions, as well as polynomial functions higher than 9 degree. Because

of the fact that 11th degree equation fulfills our needs, considering these equations is not necessary.

4. Two wheel model

A 4 wheel vehicle model with 4 degrees of freedom comprising longitudinal speed, lateral speed, angular speed and body roll rate, is still a complicated model. If the forward speed is kept constant and the roll motion is ignored, a two degree of freedom model will be sufficient. Figure 14 illustrates a two degree of freedom, two wheel model.
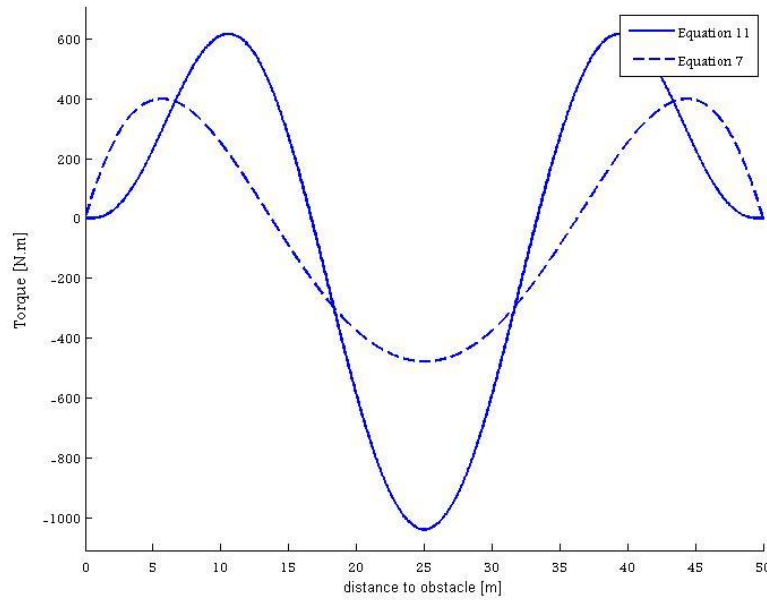
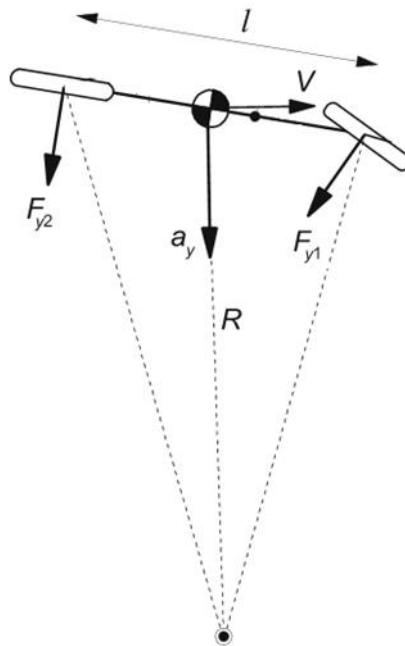**Fig7.** Moment field comparison for 7th degree and 11th degree paths

Fig8. A two degree of freedom, two wheel model

The equations of motion of the two wheel model are still nonlinear in general. Using the simple linear forms of the equations of motion the sideslip angle is obtained as,

$$\beta = \delta \left(\frac{b - \dfrac{amV^2}{lC_r}}{l - \dfrac{mV^2(aC_f - bC_r)}{lC_fC_r}} \right)$$

In the above equation, C_f and C_r are front and rear tire cornering stiffnesses. At a constant path radius R, the steer angle is,

$$\delta = \frac{1}{R}\left(a + b - mV^2 \frac{aC_f - bC_r}{(a+b)C_fC_r} \right)$$

The sideslip angle simplifies to,

$$\beta = \frac{1}{R}\left(b - \frac{amV^2}{lC_r} \right)$$

4.1. Force field

Slip is the main difference between a single mass model and two wheel model. So, there is an extra factor in two wheel model's equations. It means that equations for force field and torque field have two parts; one for a single mass model and the other one for slip. Force field and torque field values can be calculated by equations 29 to 31.

$$F_y = \left(R_iV^2 + V\frac{R_{di}}{R_i^2}q_1 \right)cos(\Psi)$$

$$F_x = \left(R_iV^2 + V\frac{R_{di}}{R_i^2}q_1 \right)sin(\Psi)$$

$$T = I_z(\ddot{y}' + \ddot{\beta}) = I_z\left(\frac{1}{L^{11}} \left(27720V^2Wx^3(L - x)^3(L - 3x)(2L - 3x) \right) + \ddot{\beta} \right)$$

Where

$$R_i = \frac{13860C}{L^{11}(A)^{1.5}}$$

$$R_{di} = \frac{L^{11}(B(L - x) - Bx)A^{0.5}}{C} + \frac{VL^{11}A^{1.5}}{6930C(L - 2x)} + \frac{VL^{11}A^{1.5}}{3465C(L - x)} - \frac{VL^{11}A^{1.5}}{3465Cx}$$

$$A = \frac{7.68e6W^2x^{10}(L - x)^{10}}{L^{22}} + 1$$

$$B = \frac{8316VW^2x^9(L - x)^9}{L^{22}}$$

$$C = Wx^4(L - x)^4(L - 2x)$$

$$q_1 = \left(b - \frac{amV^2}{(a + b)C_r} \right)$$

$$\beta = R_iq_1$$

$$\Psi = \frac{2772Wx^5(L - x)^5}{L^{11}} - \beta$$

5. Improved model

This section tries to provide an improved model for obstacle avoidance of a vehicle. The most important task is to decrease error in proportion to real results.

6-1- Analyzing primary field

A single mass model and a two wheel model have been discussed in previous chapters. Figure 15 shows lateral acceleration for a vehicle that have 75 meters distance to the obstacle and moving with 45Km/h. These results are compared for a single mass model, bicycle model and a Carsim simulation. Maximum lateral acceleration in this diagram is 1m/s2 and is almost equal for all models

Figure 16 shows vehicle rotation, which is really close to the actual values. So, when lateral acceleration is less than 1m/s2, single mass and bicycle models are efficient.

If lateral acceleration increases and exceeds 1m/s2, single mass model becomes inaccurate. The two wheel model remains useful, however it has a noticeable error compared to Carsim results. In this chapter, an improved model is suggested to provide reasonable results for less than 4m/s2 lateral acceleration.

Figures 17 and 18 compare results of a Carsim model and a field for a specific vehicle with maximum acceleration of 4 m/s2. These two figures show the difference between two wheel model and real results. According to them, two wheel model is convenient at the beginning of path, but a significant error at the end of the pass in not ignorable. This chapter follows a few solutions to decrease the error at the end of the path for a two wheel model.
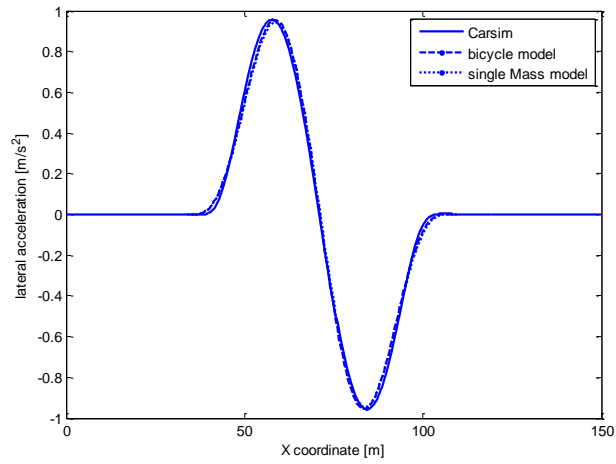
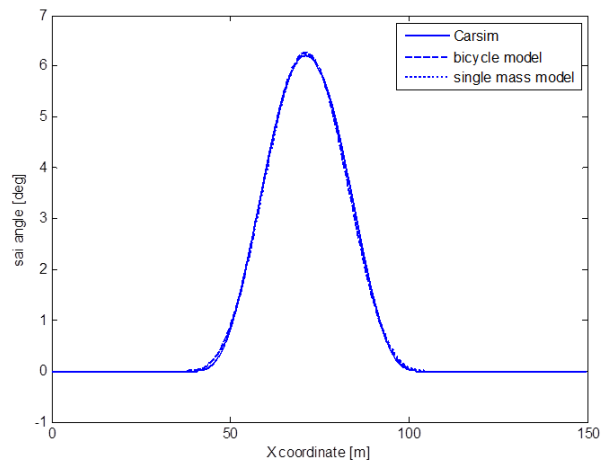**Fig9.** Lateral acceleration comparison for all models

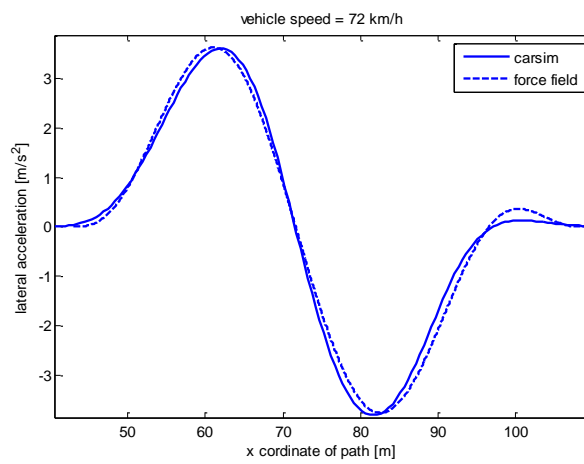**Fig10.**   Vehicle rotation angle comparison for all models

Fig11.   Vehicle lateral acceleration for a provided field and a Carsim model with maximum acceleration of 4 m/s2
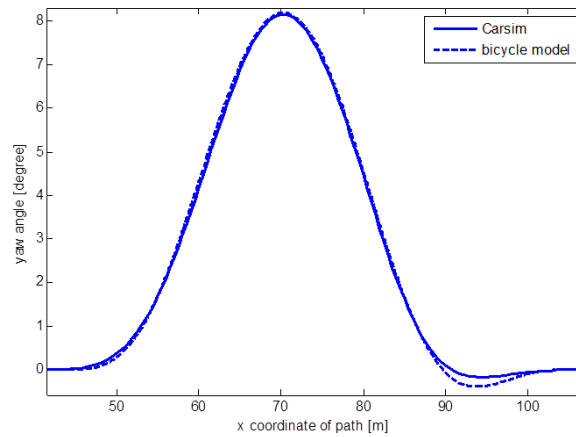
Fig12.   Vehicle lateral acceleration for a provided field and a Carsim model with maximum acceleration of 4 m/s2
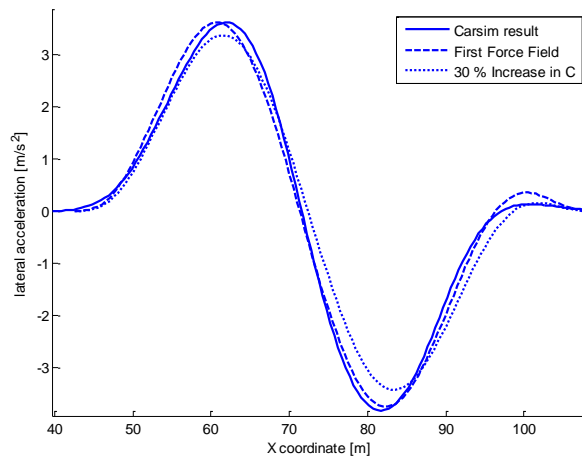

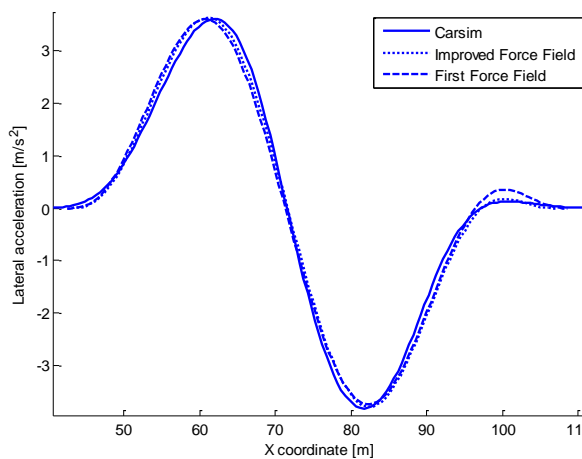**Fig13.**   effect of tire stiffness for improving provided field

Fig14.   Lateral acceleration comparison for first model, improved model and Carsim
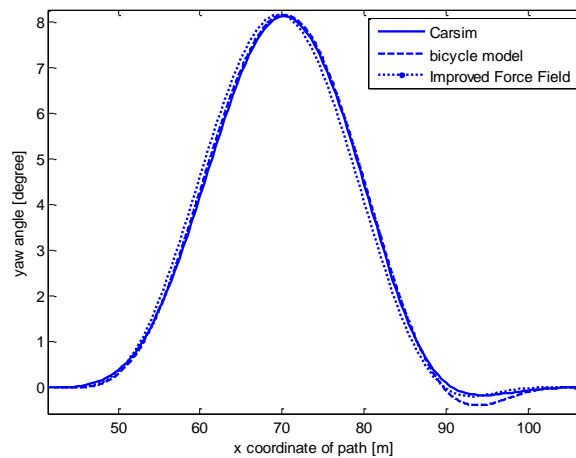
Fig15.   Yaw angle comparison for first model, improved model and Carsim

6.2. Suggested improvements

Increasing lateral slip in vehicles results in error raise and calls for improvements in provided model. Every parameter affects the force field results, so they will be investigated here.

As it has been shown in figures 17 and 18, the field has a noticeable error at the end of the path. At the end of provided field, lateral acceleration, which is equal to proportion of provided field and vehicles mass, is bigger than Carsim model. Here are three suggestions to improve the provided model based on tire stiffness.

6.2.1. First suggestion

When vehicle lateral slip in negative, increasing tire lateral stiffness cause lateral slip to decrease and as a result of that, the vehicle moves better on the path. So, first suggestion is to change the tires lateral stiffness.

Figure 19 investigates effect of a 30% raise in tire stiffness. Error at the end of the path has a major improvement but it causes problems at the rest of the path.

Adding a few coefficients (qi) into equations for lateral acceleration and yaw angle produces a better model. Some of these coefficients are added to equations by replacing x and ay with bellow equations.

$$A_y = a_y \left(q_1 + \left(\frac{q_2 x}{L} \right) \right)$$

$$X = \frac{x}{q_3}$$

Figures 20 and 21 show lateral acceleration and yaw angle for first and improved models.

6.2.2. Second suggestion

The provided field is convenient for small lateral acceleration and is inconvenient for large lateral acceleration and in this lateral accelerations, vehicle lateral slip is negative. So tire stiffness need to increase in a way that lateral slip decreases and field improves.

In this method, tire stiffness is based on longitudinal displacement in a way that is seems that tire stiffness is increasing while passing an obstacle. Tire stiffness is defined bellow

$$L = \frac{L_0}{q_1}$$

$$X = \frac{x}{q_2}$$

$$C = C_0 \left(1 + \left(\frac{x}{p_1} \right)^{p_2} \right)$$

where C0, Cr, L0 and L are lateral tire force, improved lateral tire force, vehicles distance to obstacle at the beginning and improved vehicles distance to obstacle at beginning respectively and p and q are coefficients that are calculated by try and error.

Figures 22 and 23 show lateral acceleration and yaw angle for this improved model.
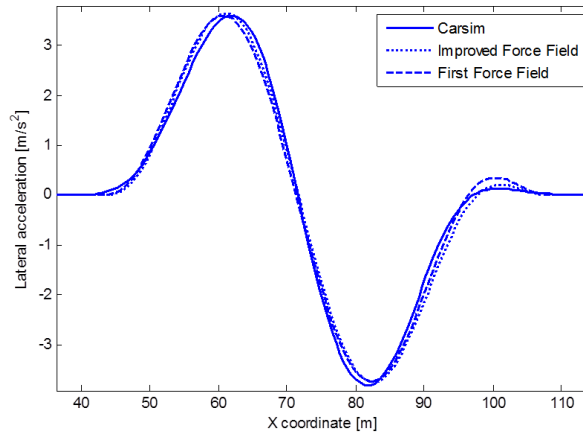
Fig16.   Lateral acceleration comparison for first model, improved model and Carsim
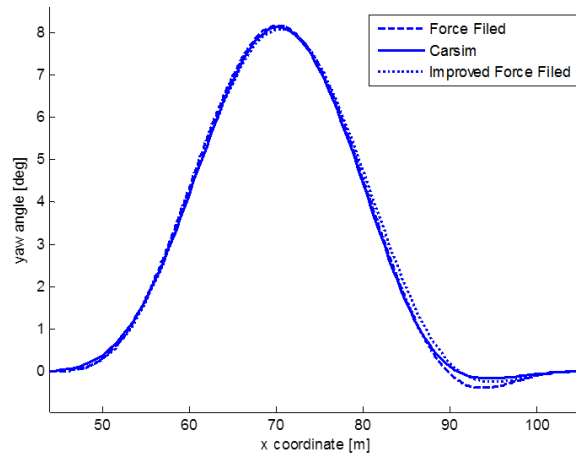

Fig17.   yaw angle comparison for first model, improved model and Carsim

6.2.2. Third suggestion

This suggestion is like the previous one with different defined equations shown here

$$C_r = p_1 C_0 (1 + \left(\frac{x}{L}\right)^{p_2})$$

$$L = L_0 - \left| \left(\frac{V}{q} - 1\right) \right|$$

These equations have been defined based on effect of each parameter on provided field. Lateral slip decreases during turn by increasing tire stiffness and result in a better field. L only affects monument field and has no effect on force field. Figures 24 and 25 show improved results for this method.

Figures 24 and 25 show that this method produces better results than others.

6.3. Final field

The third suggestion produces better results. So its results are chosen as the final model. According to the changes, final field's equations are mentioned here.

$$F_y = (R_i V^2 + V \frac{R_{di}}{R_i^2} q_1) \cos(\Psi)$$

$$F_x = (R_i V^2 + V \frac{R_{di}}{R_i^2} q_1) \sin(\Psi)$$

$$T = I_z (\frac{1}{L^{11}} \left(27720 V^2 W x^3 (L - x)^3 (L - 3x)(2L - 3x)\right) + \ddot{\beta})$$

$$R_i = \frac{13860 C}{L^{11}(A)^{1.5}}$$

$$R_{di} = \frac{L^{11}(B(L-x) - Bx)A^{0.5}}{C} + \frac{VL^{11}A^{1.5}}{6930C(L-2x)}$$

$$+ \frac{VL^{11}A^{1.5}}{3465C(L-x)} - \frac{VL^{11}A^{1.5}}{3465Cx}$$

$$A = \frac{7.68e6W^2x^{10}(L-x)^{10}}{L^{22}} + 1$$

$$B = \frac{8316VW^2x^9(L-x)^9}{L^{22}}$$

$$C = Wx^4(L-x)^4(L-2x)$$

$$q_1 = (b - \frac{amV^2}{(a+b)C_r})$$

$$\beta = R_i q_1$$

$$\Psi = \frac{2772Wx^5(L-x)^5}{L^{11}} - \beta$$

$$C_r = p_1 C_0 (1 + \left(\frac{x}{L}\right)^{p_2})$$

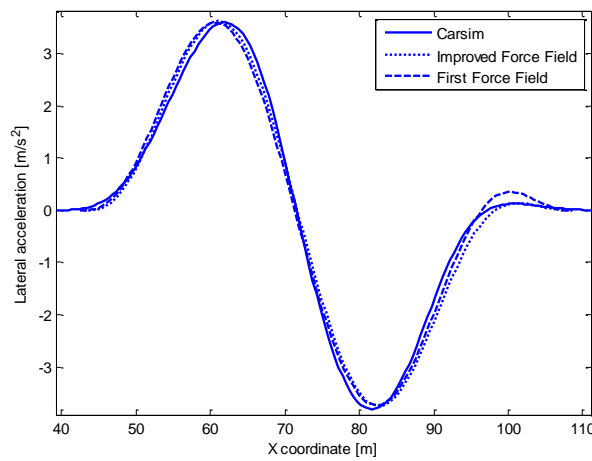$$L = L_0 - \left|(\frac{V}{q} - 1)\right|$$

Fig18.   Lateral acceleration comparison for first model, improved model and Carsim
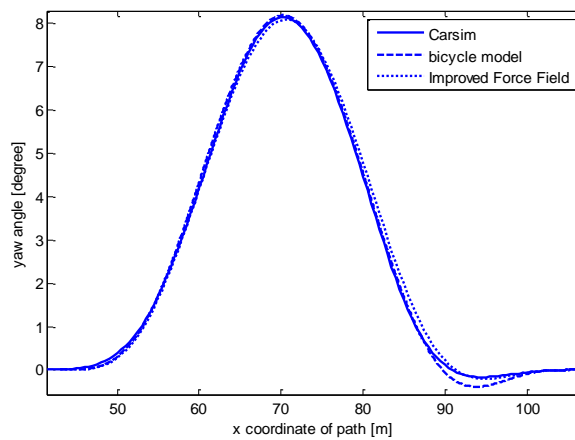

Fig19.   yaw angle comparison for first model, improved model and Carsim

6. Conclusion

Every vehicle needs to pass through multiple obstacles on its way. So, this paper tries to guide vehicles using force field method. First of all, this paper describes motion constrains and lane change conditions. After that an 11th degree equation was chosen as vehicles path. For moving on the chosen path, an appropriate steer angle is required as input. This steer angle produces lateral slip in tiers. Tire models can calculate lateral forces but these models result in nonlinear equations which is not desirable.

4, 3 and two degree of freedom models are common for simulating vehicles handling and lane change. In this paper, vehicles longitudinal speed assumed to be constant. So, the 3 degree of freedom model is errorless. However, 3 degree of freedom equations are nonlinear and mass and stiffness matrixes are coupled. As a result of that, analytical solution is impossible and numerical solution is needed. So, steady state tow degree of freedom model was chosen here.

A simple single mass model is presented in chapter 3. In this model, the vehicle has a specific mass and moment of inertia and its governing equations are independent. After presenting the elementary model and analyzing its pros and cones, a two wheel models is presented considering effects of slip. This method had some malfunctions which are identified by comparing it with real results of Carsim. Identifying primary models defects leads to an improved model which was presented in chapter 6 for negative lateral slips, lateral slip increaser toward zero by increasing tire stiffness. At the end, 3 ideal were suggested to adjust tire stiffness.

References

[1]. Vahidi, Ardalan, and Azim Eskandarian. "Research advances in intelligent collision avoidance and adaptive cruise control." Intelligent Transportation Systems, IEEE Transactions on 4.3 (2003): 143-153.

[2]. Kawazoe, Hiroshi, et al. "Development of a lane-keeping support system". No. 2001-01-0797. SAE Technical Paper, 2001.

[3]. Chen, Chieh, and Han-Shue Tan. "Steering control of high speed vehicles: dynamic look ahead and yaw rate feedback." Decision and control, 1998. Proceedings of the 37th IEEE conference on. Vol. 1. IEEE, 1998.

[4]. Guldner, Jurgen, et al. "Robust automatic steering control for look-down reference systems with front and rear sensors." Control Systems Technology, IEEE Transactions on 7.1 (1999): 2-11.

[5]. Akar, Mehmet, and Jens C. Kalkkuhl. "Lateral dynamics emulation via a four-wheel steering vehicle." Vehicle System Dynamics 46.9 (2008): 803-829.

[6]. Hatipoglu, Cem, Ümit Özgüner, and Keith A. Redmill. "Automated lane change controller design." Intelligent Transportation Systems, IEEE Transactions on 4.1 (2003): 13-22.

[7]. Akar, Mehmet, and Jens C. Kalkkuhl. "Lateral dynamics emulation via a four-wheel steering vehicle." Vehicle System Dynamics 46.9 (2008): 803-829.

[8]. Nagai, M., H. Mouri, and P. Raksincharoensak. "Vehicle lane-tracking control with steering torque input." Vehicle System Dynamics 37 (2003): 267-278.

[9]. Ryu, Jeha, Ho-Soo Kim, and Jong-Hyup Kim. "An emergency obstacle avoidance control strategy for automated highway vehicles." Vehicle System Dynamics 38.5 (2002): 319-339.

[10]. Anderson, Sterling J., et al. "An optimal-control-based framework for trajectory planning, threat assessment, and semi-autonomous control of passenger vehicles in hazard avoidance scenarios." International Journal of Vehicle Autonomous Systems 8.2-4 (2010): 190-216.

[11]. Keviczky, Tamás, et al. "Predictive control approach to autonomous vehicle steering." American Control Conference, 2006. IEEE, 2006.

[12]. Shiller, Zvi, and Satish Sundar. "Emergency lane-change maneuvers of autonomous vehicles." Journal of dynamic systems, measurement, and control 120.1 (1998): 37-44.

[13]. Hattori, Yoshikazu, Eiichi Ono, and Shigeyuki Hosoe. "Optimum vehicle trajectory control for obstacle avoidance problem." Mechatronics, IEEE/ASME Transactions on 11.5 (2006): 507-512.

[14]. Bevan, G. P., H. Gollee, and J. O'Reilly. "Trajectory generation for road vehicle obstacle avoidance using convex optimization." Proceedings of the Institution of Mechanical Engineers, Part D: Journal of Automobile Engineering 224.4 (2010): 455-473.

[15]. Koren, Yoram, and Johann Borenstein. "Potential field methods and their inherent limitations for mobile robot navigation." Robotics and Automation, 1991. Proceedings., 1991 IEEE International Conference on. IEEE, 1991.

[16]. Zhang, Qiushi, Dandan Chen, and Ting Chen. "An obstacle avoidance method of soccer robot based on evolutionary artificial potential field."Energy Procedia 16 (2012): 1792-1798.

[17]. Huang, Wesley H., et al. "Visual navigation and obstacle avoidance using a steering potential function." Robotics and Autonomous Systems 54.4 (2006): 288-299.

[18]. Song, Qiang, and Lingxia Liu. "Mobile robot path planning based on dynamic fuzzy artificial potential field method." International Journal of Hybrid Information Technology 5.4 (2012): 85-94.

[19]. Adeli, Hossein, et al. "Path planning for mobile robots using iterative artificial potential field method." IJCSI International Journal of Computer Science Issues 8.4 (2011).

[20]. Li, Guanghui, et al. "An efficient improved artificial potential field based regression search method for robot path planning." Mechatronics and Automation (ICMA), 2012 International Conference on. IEEE, 2012.

[21]. Sfeir, Joe, Maarouf Saad, and Hamadou Saliah-Hassane. "An improved artificial potential field approach to real-time mobile robot path planning in an unknown environment." Robotic and Sensors Environments (ROSE), 2011 IEEE International Symposium on. IEEE, 2011.

[22]. Hong, Zhang, et al. "The dynamic path planning research for mobile robot based on artificial potential field." Consumer Electronics, Communications and Networks (CECNet), 2011 International Conference on. IEEE, 2011.

[23]. Daily, Robert, and David M. Bevly. "Harmonic potential field path planning for high speed vehicles." American Control Conference, 2008. IEEE, 2008.

[24]. Lee, Min Cheol, and Min Gyu Park. "Artificial potential field based path planning for mobile robots using a virtual obstacle concept." Advanced Intelligent Mechatronics, 2003. AIM 2003. Proceedings. 2003 IEEE/ASME International Conference on. Vol. 2. IEEE, 2003.

[25]. Hwang, Yong K., and Narendra Ahuja. "A potential field approach to path planning." Robotics and Automation, IEEE Transactions on 8.1 (1992): 23-32.

[26]. Ge, Shuzhi S., and Yun J. Cui. "Dynamic motion planning for mobile robots using potential field method." Autonomous Robots 13.3 (2002): 207-222.